# SUPPLEMENTARY MATERIAL FOR "TUNABLE INTERACTION BETWEEN METAL CLUSTERS AND GRAPHENE"

## A. Binding energies

TABLE I. Binding energy ($E_b$) of 6-atom metal clusters and graphene layers (Eq. 1). The different cases correspond the case of defect-free (DFG) and different positions on a graphene layer containing a SWD. The values presented corresponding to LDA calculations.

| Binding energy $E_b$ (eV) | | | | | |
|---|---|---|---|---|---|
| Cluster | **DFG** | **SWD-A** | **SWD-B** | **SWD-C** | **SWD-D** |
| **Ti**$_6$ | 5.1 | 5.9 | 7.0 | 5.9 | 6.8 |
| **Pd**$_6$ | 3.0 | 4.0 | 4.1 | 4.0 | 4.1 |
| **Pt**$_6$ | 2.8 | 4.6 | 4.4 | 4.6 | 3.9 |
| **Au**$_6$ | 1.1 | 1.5 | 1.9 | 1.6 | 1.6 |

The binding energies $E_b$ between the TM clusters and the graphene sheet were calculated using:

$$E_b = E_{tot}[M] + E_{tot}[G] - E_{tot}[G + M], \tag{1}$$

where $E_{tot}[M]$, $E_{tot}[G]$ and $E_{tot}[G + M]$ represent total energy of the isolated metal cluster, isolated graphene layer and combined cluster-graphene layer system, respectively. The binding energy results are computed for the different TM clusters and the different configurations of the interacting system.

## I. GEOMETRIC STRUCTURES

Figures 1 and 2 show the top and side views of 6-atom clusters on pristine graphene, and on graphene with a Stone-Wales defect, respectively. These structures have been obtained through a conjugated-gradient optimization procedure using the LDA approximation to the exchange and correlation functional.

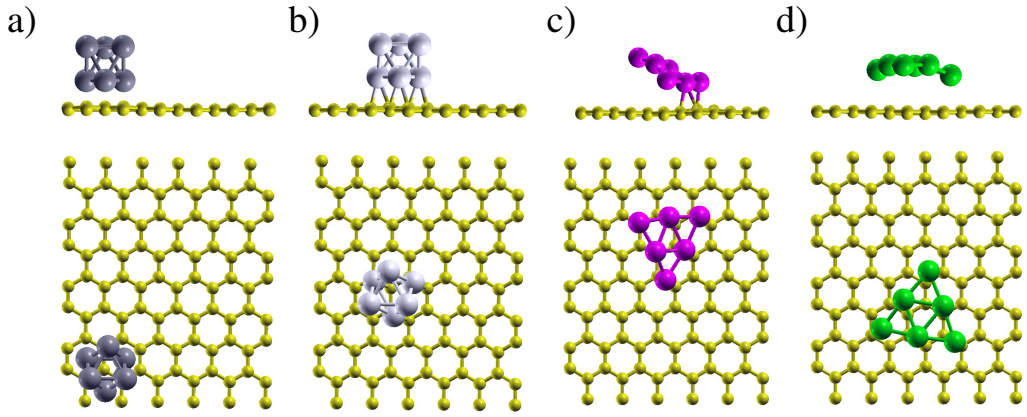


FIG. 1. (Color online) (LDA results) Top and side view of relaxed structures corresponding to: (a) $Ti_6$ on pristine graphene; (b) $Pd_6$ on pristine graphene; (c) $Pt_6$ on pristine graphene; (d) $Au_6$ on pristine graphene;

Figures 3 and 4 show the top and side views of 6-atom clusters on pristine graphene, and on graphene with a Stone-Wales defect, respectively, using the GGA approximation to the exchange and correlation functional.

The band structures of different combined systems are analyzed to gain further insight on the interaction between the metal clusters and graphene. The cases of 6-atom clusters placed in different positions of the layer are presented in rows of Fig. 5 (from top to bottom): defect-free graphene (DFG), away from the defect (SWD-A) and on the pentagon site of the defect (SWD-B). The decomposition of the Bloch states onto the $s$ (red) and $d$ (blue) atomic orbitals of

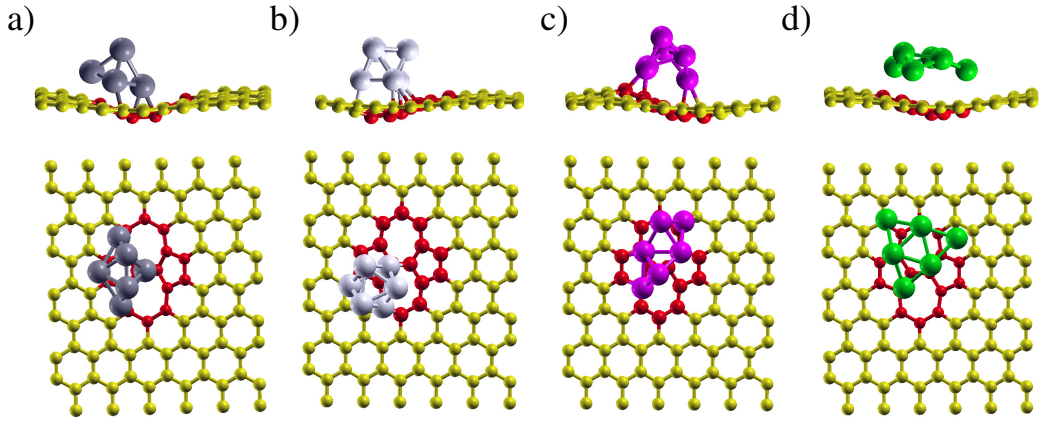


FIG. 2. (Color online) (LDA results) Top and side view of relaxed structures corresponding to: (a) $Ti_6$ on graphene with SWD; (b) $Pd_6$ on graphene with SWD; (c) $Pt_6$ on graphene with SWD; (d) $Au_6$ on graphene with SWD; The carbon atoms near the defect have been colored differently to ease visualization.

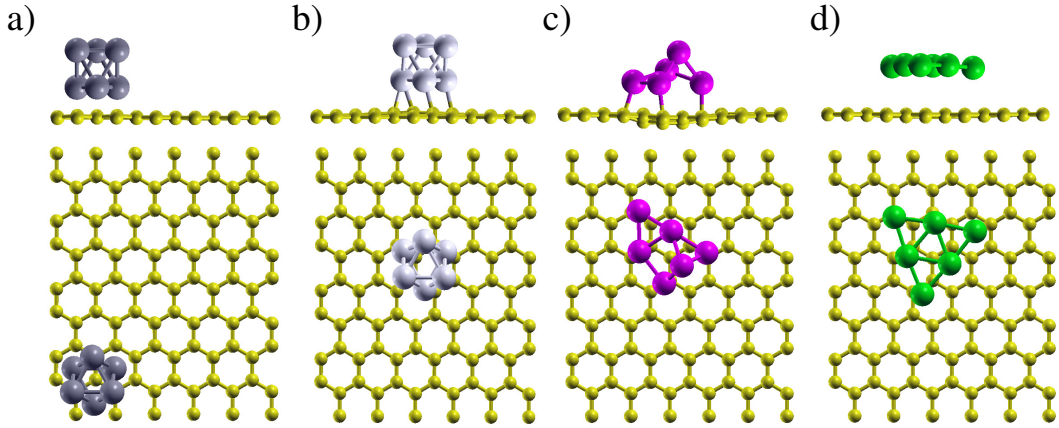


FIG. 3. (Color online) (GGA results) Top and side view of relaxed structures corresponding to: (a) $Ti_6$ on pristine graphene; (b) $Pd_6$ on pristine graphene; (c) $Pt_6$ on pristine graphene; (d) $Au_6$ on pristine graphene;

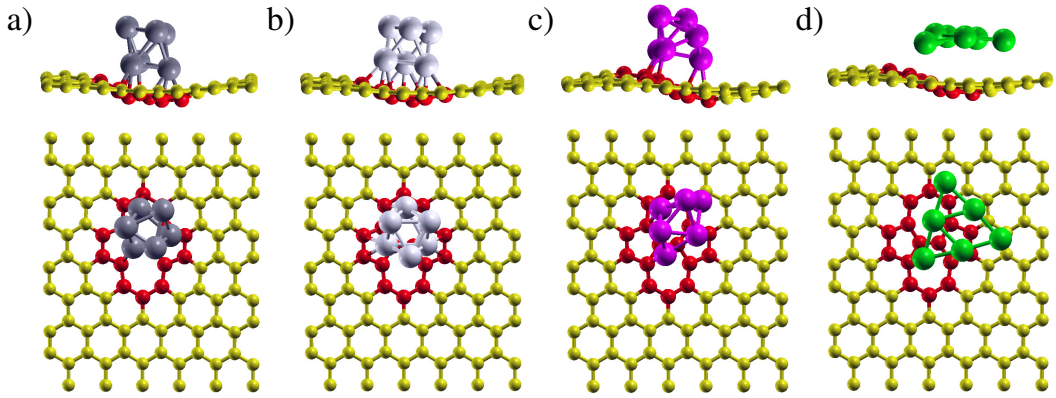


FIG. 4. (Color online) (GGA results) Top and side view of relaxed structures corresponding to: (a) $Ti_6$ on graphene with SWD; (b) $Pd_6$ on graphene with SWD; (c) $Pt_6$ on graphene with SWD; (d) $Au_6$ on graphene with SWD; The carbon atoms near the defect have been colored differently to ease visualization.

the TM cluster is plotted in the figure. The band structures of interacting systems revealed spin-polarization for $Ti_6$, $Pd_6$ and $Pt_6$ on graphene layers, which is absent for the $Au_6$/graphene case.

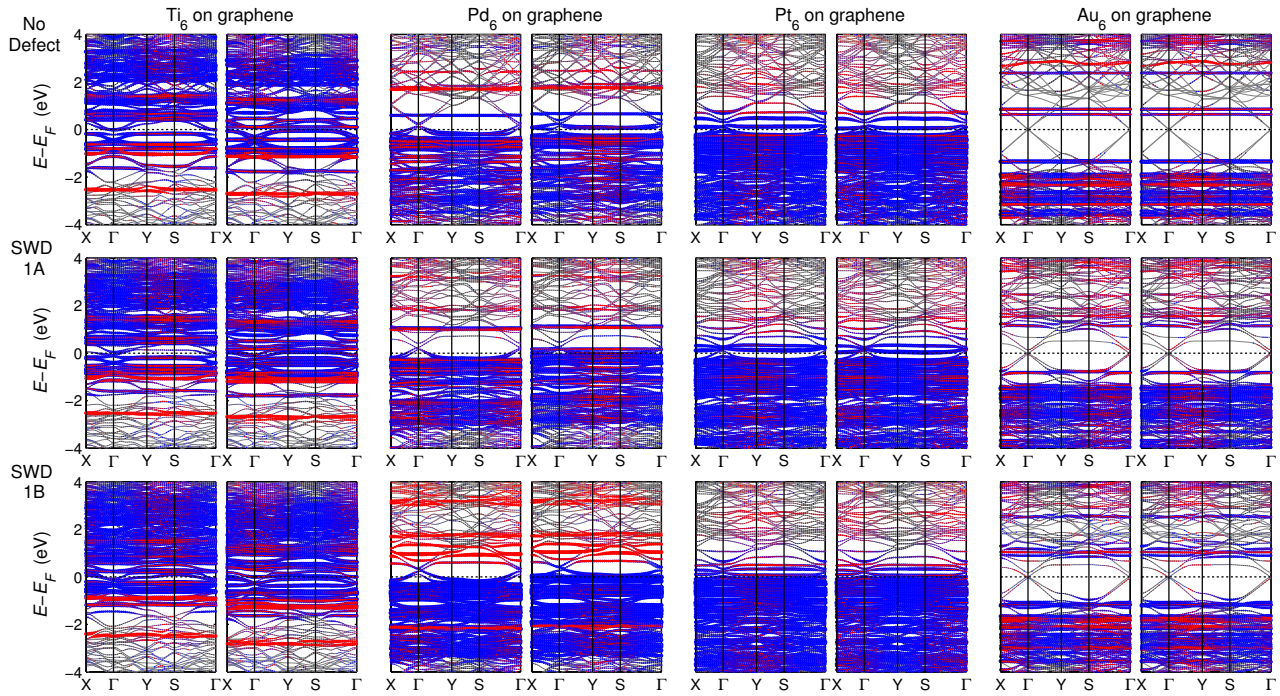


FIG. 5. Band structure (grey lines) of different TM cluster at various positions on graphene layers (from left to right): $Ti_6$, $Pd_6$, $Pt_6$, and $Au_6$. Different rows correspond to pristine graphene (top), away from the SWD (middle), and on top of the SWD (bottom). The blue and red colored bands correspond to projections onto localized atomic *d*-orbitals and *s*-orbitals of the TM atoms, respectively.

Fig. 6 shows the ground state structures for the 13-atom clusters used in this work. These structures were obtained in a previous work by one of the authors.[1]

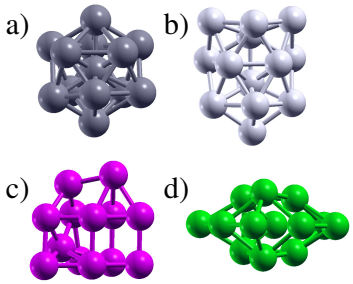


FIG. 6. (Color online)
The ground state structures of the 13-atom TM clusters, as obtained in a previous work[1]. (a) $Ti_{13}$ exhibits a distorted icosahedral symmetry; (b) $Pd_{13}$ has a distorted hexagonal bilayer structure; (c) $Pt_{13}$ presents a double simple cubic structure, and (d) $Au_{13}$ the disordered structure.

Figures 7 and 8 show the top and side views of 13-atom clusters on graphene with a Stone-Wales defect, and on pristine graphene, respectively, using the GGA-PBE approximation to the exchange and correlation functional.

Finally, Fig.9 shows the minimum energy configurations found for the 6-atom clusters on graphene with a 555-777 defect, using the GGA-PBE approximation to the exchange and correlation functional.

---

[1] M. Piotrowski, P. Piquini, and J. Da Silva, Physical Review B **81**, 155446 (2010).

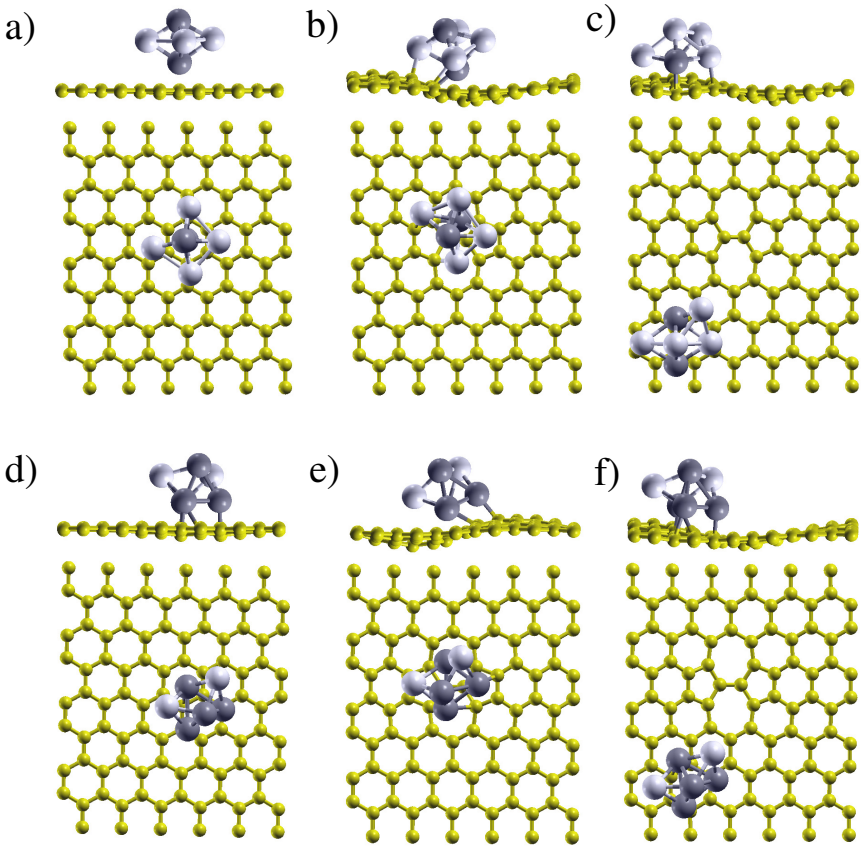


FIG. 7. (Color online) Top and side views of the optimized structures corresponding to 6-atom clusters on pristine graphene and with SWD. $Ti_2Pd_4$ on pristine graphene (a), on defect SWD position B (b) and position A. d) $Ti_4Pd_2$ on pristine graphene and with SWD e) on position B and f) position A on graphene layer.

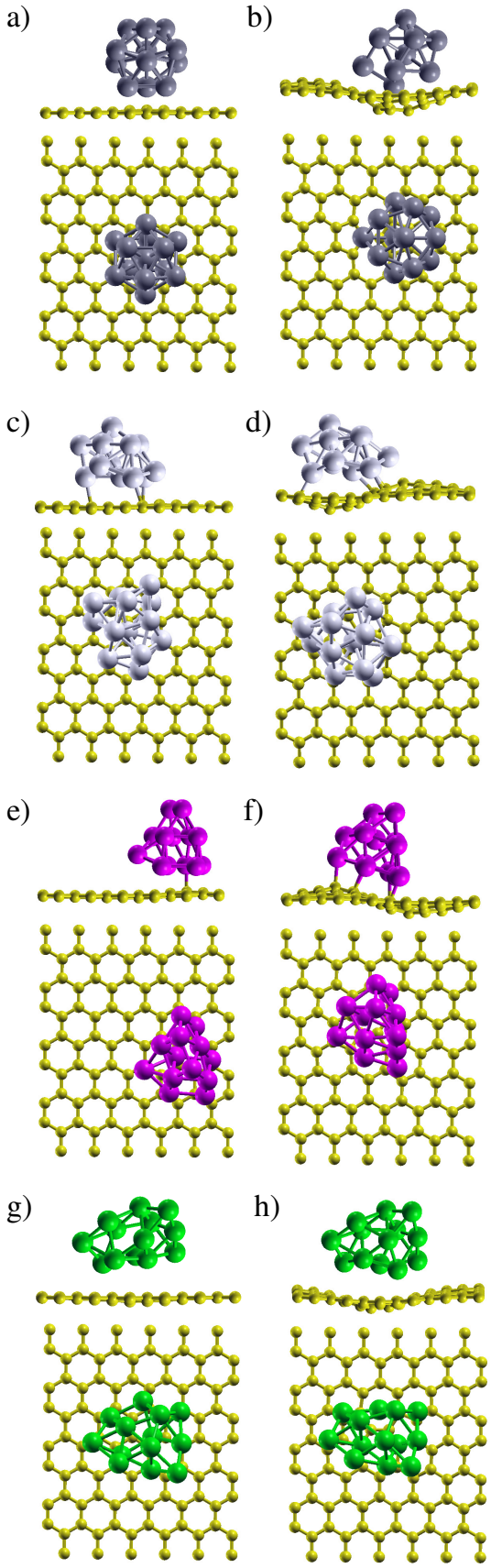


FIG. 8. (Color online)
Top and site views of optimized structures corresponding to the pristine graphene interacting with (a) Ti, (c) Pd, (e) Pt and (g) Au 13-atom clusters. on graphene with SWD (b), (d), (f) and (h).

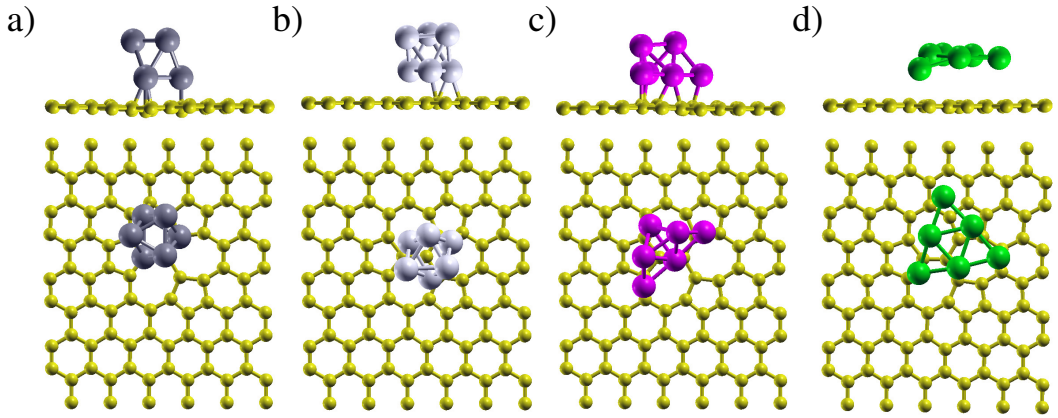


FIG. 9. (Color online) Top and side views of optimized structures corresponding to 6-atom clusters on graphene and with SWD (555-777).